

RESEARCH

Open Access



Role of interatrial block in modulating cryptogenic stroke risk in patients with patent foramen ovale: a retrospective study

Ye Du¹, Yanxing Zhang¹, Yangbo Xing², Xiatian Liu³, Huayong Jin⁴, Yuxin Zhang⁵, Chengyi Li⁶ and Buyun Xu^{2*}

Abstract

Background The patent foramen ovale (PFO) and interatrial block (IAB) are associated with cryptogenic stroke (CS). However, the role of the interaction between PFO and IAB in CS remains unclear.

Methods This case–control study enrolled 256 patients with CS and 156 individuals without a history of stroke or transient ischemic attack. IAB was defined as P wave duration > 120 ms. PFO was evaluated by contrast transesophageal echocardiography, and classified as no-PFO, low-risk PFO and high-risk PFO. Multiplicative and additive interaction analysis were used to assess the interaction between PFO and IAB in CS.

Results Multiplicative interaction analysis unveiled a significant interaction between IAB and low-risk PFO in CS (OR for interaction = 3.653, 95% CI, 1.115–12.506; $P=0.037$). Additive interaction analysis indicated that 68.4% (95% CI, 0.333–1.050; $P<0.001$) of the increased risk of CS related to low-risk PFO was attributed to the interaction with IAB. The results were robust in multivariate analysis. However, but no significant multiplicative or additive interaction was observed between IAB and high-risk PFO. When stratified by IAB, high-risk PFO was associated with CS in both patients with IAB (OR, 4.186; 95% CI, 1.617–10.839; $P=0.003$) and without IAB (OR, 3.476; 95% CI, 1.790–6.750; $P<0.001$). However, low-risk PFO was only associated with CS in patients with IAB (OR, 2.684; 95% CI, 1.007–7.149; $P=0.048$) but not in those without IAB (OR, 0.753; 95% CI, 0.343–1.651; $P=0.479$).

Conclusion The interaction between IAB and PFO might play an important role in CS, particularly in cases with low-risk PFO.

Keyword Patent foramen ovale, interatrial block, cryptogenic strokes, ischemic stroke

*Correspondence:

Buyun Xu
xbyzju@zju.edu.cn

¹ Department of Neurology, Shaoxing People's Hospital (Shaoxing Hospital, Zhejiang University School of Medicine), Shaoxing 312000, China

² Department of Cardiology, Shaoxing People's Hospital (Shaoxing Hospital, Zhejiang University School of Medicine), 568 # Zhongxing North Road, Shaoxing, Zhejiang Province 312000, China

³ Department of Ultrasound, Shaoxing People's Hospital (Shaoxing Hospital, Zhejiang University School of Medicine), Shaoxing 312000, China

⁴ Department of Electrocardiogram, Shaoxing People's Hospital (Shaoxing Hospital, Zhejiang University School of Medicine), Shaoxing 312000, China

⁵ Zhejiang University School of Medicine, Hangzhou 310000, China

⁶ Shaoxing University School of Medicine, Shaoxing 312000, China



© The Author(s) 2024. **Open Access** This article is licensed under a Creative Commons Attribution-NonCommercial-NoDerivatives 4.0 International License, which permits any non-commercial use, sharing, distribution and reproduction in any medium or format, as long as you give appropriate credit to the original author(s) and the source, provide a link to the Creative Commons licence, and indicate if you modified the licensed material. You do not have permission under this licence to share adapted material derived from this article or parts of it. The images or other third party material in this article are included in the article's Creative Commons licence, unless indicated otherwise in a credit line to the material. If material is not included in the article's Creative Commons licence and your intended use is not permitted by statutory regulation or exceeds the permitted use, you will need to obtain permission directly from the copyright holder. To view a copy of this licence, visit <http://creativecommons.org/licenses/by-nc-nd/4.0/>.

Introduction

Stroke is a significant contributor to global mortality and disability, of which 70% can be attributed to ischemic stroke (IS). It is essential to understand the mechanisms underlying IS for its secondary prevention. However, the etiology is undetermined in approximately 25% of IS cases, which are categorized as cryptogenic stroke (CS) [1].

Recently, the role of the patent foramen ovale (PFO) in IS has gained significant attention. PFO-related strokes account for 5% of all stroke cases and up to 10% in younger patients [1]. Randomized controlled trials have demonstrated the efficacy of PFO closure in preventing CS, reinforcing the significant role of the PFO in stroke etiology [1]. Paradoxical embolism is deemed the primary mechanism by which PFO contributes to IS [2], whereas other mechanisms, such as in situ thrombus formation [3], atrial arrhythmias, and reduced left atrial function, may also play a role in PFO-associated stroke [4]. In addition to PFO, interatrial block (IAB) is supposedly associated with IS [5]. IAB not only correlates with atrial fibrillation (AF) [5], but also increases the risk of IS in patients without AF, potentially due to left atrial blood stasis induced by IAB [5, 6].

However, limited studies have focused on the relationship between the PFO and IAB and the role of their interactions on IS risk. The present study aimed to investigate the association between PFO and IAB and elucidate the impact of the interaction between PFO and IAB on CS risk.

Materials and methods

This case-control study was conducted in compliance with the ethical standards of the corresponding institution and the Declaration of Helsinki. The ethics review boards of Shaoxing People's Hospital approved this study, and the requirement for informed consent was waived owing to the retrospective nature of this study. The analysis was reported in accordance with the STROBE guidelines.

Study population

For the cryptogenic stroke group (CS group), we consecutively enrolled patients with CS aged between 18 and 75 years, who underwent contrast transesophageal echocardiography (cTEE) at the Shaoxing People's Hospital from January 2021 to December 2023. The diagnosis of CS was adjudicated by cardiologists and neurologists based on previously published criteria [7]. All stroke cases were confirmed by brain magnetic resonance imaging and neurologic examination. The following tests were performed in all patients: transthoracic echocardiography and TEE; extracranial artery ultrasound or computed

tomography angiography; laboratory tests; 12-lead electrocardiography; and 24-h Holter electrocardiographic monitoring. Patients with incomplete evaluations were not considered to have CS.

The control group comprised consecutive patients without a history of stroke/transient ischemic attack (TIA) who underwent cTEE at the Shaoxing People's Hospital during the same period.

The exclusion criteria were as follows: 1) atrial fibrillation/flutter or sustained atrial tachycardia (> 30 s); 2) atrial premature beats within a 24-h period exceeding 10,000; 3) without electrocardiography results within 1 year before IS or cTEE; 4) valvular heart disease, congenital heart disease other than PFO, or cardiomyopathy; 5) heart failure stages C to D [8]; 6) left atrial anteroposterior diameter greater than 45 mm; 7) a history of stroke or TIA; 8) systemic inflammatory diseases, coagulation dysfunction or malignancies; 9) PFO-related diseases other than IS, such as migraines and decompression sickness; and 10) missing key information or other conditions deemed unsuitable for inclusion by investigators.

Electrocardiography and echocardiography measurements

The last patients' ECGs within 1 year before IS or cTEE were obtained electronically. P-wave durations were measured using the MUSE v9 Cardiology Information System (GE HealthCare, UK). IAB was defined as a prolonged P-wave duration (≥ 120 ms) in the inferior leads [6]. The ECGs were analyzed by an independent experienced electrocardiologist blinded to the patients' information.

All c-TEE examinations were performed according to local clinical protocols published previously [9]. A Philips EPIQ 7C real-time three-dimensional color cardiac ultrasound system (Philips Ultrasound, Bothell, Washington, United States) equipped with a transesophageal three-dimensional matrix probe X8-2t (frequency, 2–8 MHz) was utilized for the examinations. The contrast agent used was an agitated saline solution, administered via the antecubital vein. Images of each chamber section were observed both at rest and after a Valsalva maneuver, capturing at least 20 cardiac cycles. PFO was confirmed when the channel was visibly open and microbubbles traversed from the right to the left atrium within three cardiac cycles subsequent to right atrium opacification. All images were stored in a database and assessed by an experienced sonographer blinded to the patients' information.

The following characteristics of PFO were evaluated: the grading of right-to-left shunt flow (RLS), PFO size, atrial septal aneurysm (ASA) and hypermobile septum. All characteristics were evaluated at rest, except for RLS,

which was evaluated both at rest and after the Valsalva maneuver.

The PFO with a right-to-left shunt (PFO-RLS) typically manifests within the initial 3–6 cardiac cycles following right atrium opacification. PFO-RLS was graded as follows: grade 0, the absence of microbubbles; grade 1, the presence of 1–10 microbubbles; grade 2, the presence of 11–30 microbubbles; and grade 3, the occurrence of >30 microbubbles or near-complete opacification of the left atrium. The PFO height was measured as the maximum separation between the septum primum and septum secundum in the end-systolic frame, and a large-size PFO was defined as a PFO with a height exceeding 2 mm. ASA was characterized by >10 mm septal excursion from the midline into the right or left atrium, or >15 mm total excursion between both atria. Additionally, a moving and floppy septum, defined as >5 mm septal excursion in every heartbeat, was categorized as a hypermobile interatrial septum [10].

The PFO with at least one of the following characteristics was defined as a high-risk PFO: PFO-RLS grade >2 at rest or after the Valsalva maneuver, a large-size PFO, ASA or a hypermobile septum. Otherwise, the PFO was defined as low-risk PFO [4, 7].

Data collection

The patients' medical history was retrieved from medical records. To avoid the impact of IS on laboratory test results, the laboratory tests performed after the acute stage (1–2 weeks) of IS were abstracted for analysis. In the control group, the laboratory tests were conducted within 1 week before or after the cTEE procedure.

Statistical analyses

The Kolmogorov–Smirnov test was utilized to evaluate the normal distribution of continuous variables. Normally distributed data are presented as mean \pm standard deviation and were compared using the Student's *t*-test. Skewed data are expressed as median (lower quartile–upper quartile) and were compared using the Mann–Whitney test. Categorical variables are presented as counts and were compared using the Fisher's exact test or Pearson's chi-squared test, as appropriate.

The association between CS and potential risk factors was estimated by odds ratios (ORs) with 95% confidence intervals (CIs) calculated by logistic regression. Multiplicative and additive methods were used to investigate the role of interaction between IAB and PFO in CS development. Multiplicative interaction was assessed by introducing an interaction term into the logistic regression models. Additive methods were used to calculate the following parameters: 1) the attributable proportion (AP); 2) the relative excess risk due to interaction (RERI); and

3) the synergy index (SI) [11]. Moreover, subgroup analyses were conducted to evaluate the roles of IAB and PFO in CS development.

All data analyses were performed using R version 4.2.0. The “InteractionR” package was utilized for conducting interaction analyses. Statistical significance was determined at a 2-sided *p*-value ≤ 0.05 .

Results

Characteristics of study population

During the study, 304 patients with CS and 329 individuals without stroke/TIA underwent cTEE and ECG. We excluded 221 participants based on the exclusion criteria. Finally, 412 participants were included in the analysis. Figure 1 illustrates the participant selection process. Of the participants, 256 had CS (CS group) and the remaining 156 were classified as the control group. Participants in the CS group were older (56.7 ± 9.7 vs. 53.7 ± 13.0 years, $P=0.014$) and predominantly comprised men (68.0% vs. 54.5%, $P=0.006$), drinker (37.5% vs. 25.0%, $P=0.009$) and smokers (29.7% vs. 20.5%, $P=0.040$). Moreover, the incidences of hypertension (60.5% vs. 35.9%, $P<0.001$) and diabetes (21.1% vs. 7.7%, $P<0.001$) were significantly higher in the CS group. Additionally, patients in the CS group exhibited lower high-density lipoprotein (HDL) levels, larger left atrial dimensions, longer P-wave durations, and a higher IAB incidence. Regarding PFO, high-risk PFO incidence was higher in the CS group (34.8% vs. 13.5%, $P<0.001$), whereas there was no significant difference in low-risk PFO incidence between the groups (14.8% vs. 15.4%, $P=0.849$). Among patients with PFO, the PFO size was larger in the CS group (2.59 ± 1.37 vs. 1.99 ± 0.85 mm, $P=0.001$), while the RLS grade and incidence of ASA and hypermobile septa were comparable between the groups. Table 1 summarizes the characteristics of the participants. Table 2 presents the morphometric and functional characteristics of the PFO.

Risk of cryptogenic strokes and interaction of IAB and PFO

In the univariate analysis, conventional risk factors, such as age, sex, alcohol, smoking, hypertension, diabetes, D-dimer levels, high density lipoprotein levels and left atrial size, showed associations with CS. In addition, IAB (OR, 1.961; 95% CI, 1.293–2.973; $P=0.002$) and high-risk PFO (OR, 3.647; 95% CI, 2.127–6.251; $P<0.001$) were also associated with CS, whereas low-risk PFO (OR, 1.362; 95% CI, 0.770–2.410; $P=0.288$) displayed no association. Regarding to PFO characteristics, PFO size was the only factor associated with CS. Tables S1-2 show the results of the univariate analysis. After adjustment for potential confounders, the association between IAB, high-risk PFO, and CS remained significant (Table 3).

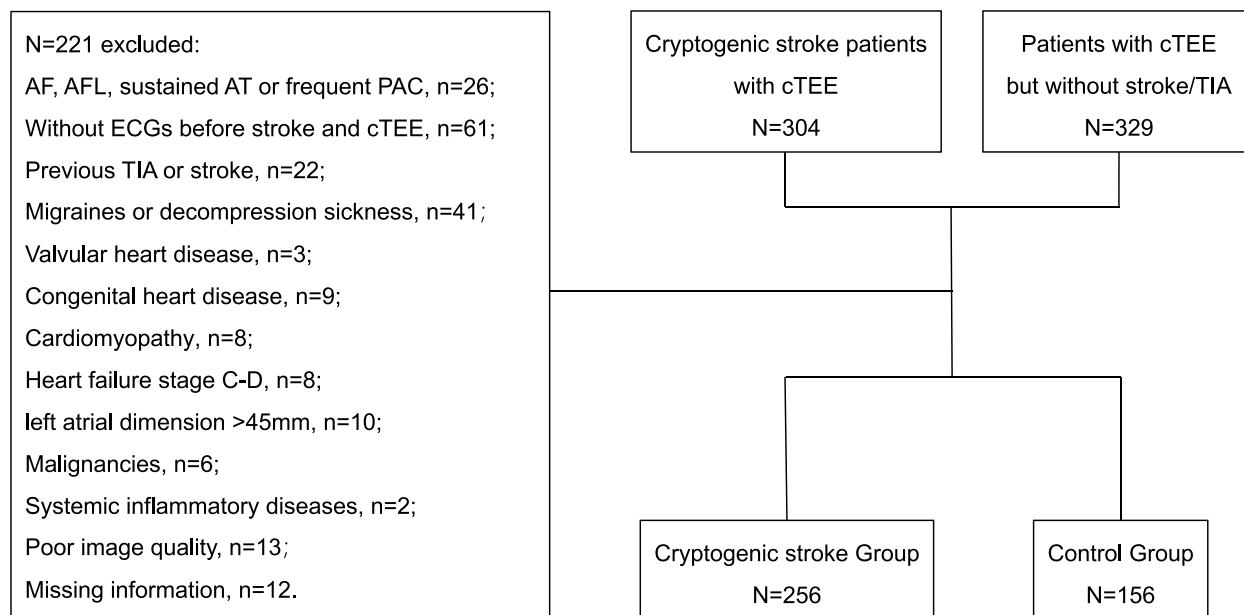


Fig. 1 Patients' selection process. AF, atrial fibrillation; AFL, atrial flutter; AT, atrial tachycardia; cTEE, contrast transesophageal echocardiography; PAC, premature atrial complex; TIA, transit ischemic attack

Before evaluating the interaction, the relationship between PFO and IAB was investigated. The incidence of IAB was comparable among participants with low-risk PFO, high-risk PFO, and those without PFO (31/62 vs. 45/110 vs. 97/240, $P=0.381$). Among participants with PFO, no association was detected between IAB and PFO characteristics (Table S3).

Multiplicative interaction analysis unveiled a significant interaction between IAB and low-risk PFO (OR for interaction = 3.653, 95% CI, 1.115–12.506; $P=0.037$), while no significant multiplicative interaction was observed between IAB and high-risk PFO (OR for interaction = 1.204, 95% CI, 0.378–3.841; $P=0.753$). Regarding additive interaction analysis, a significant AP of 0.684 (95%CI, 0.333–1.050; $P<0.001$) was observed for IAB and low-risk PFO upon using no-IAB/no-PFO as the comparator. Correspondingly, the RERI ($P=0.073$) and SI ($P=0.079$) tended to be significant. However, no significant AP, RERI and SI were detected for IAB and high-risk PFO (Table 4). The results of the interaction analysis remained robust after adjusting for potential confounders, as depicted in Table 4. In the subgroup analysis, IAB conferred an increased risk of CS in patients with low-risk PFO (OR, 5.769; 95% CI, 1.843–18.064; $P=0.003$) and tended to increase CS risk in patients without PFO (OR, 1.619; 95% CI, 0.960–2.732; $P=0.071$). However, no significant association between IAB and CS was detected in patients with high-risk PFO (OR, 1.950; 95% CI, 0.693–5.491; $P=0.206$). When stratified by IAB, high-risk PFO

was associated with CS in both patients with IAB (OR, 4.186; 95% CI, 1.617–10.839; $P=0.003$) and without IAB (OR, 3.476; 95% CI, 1.790–6.750; $P<0.001$). However, low-risk PFO was only associated with CS in patients with IAB (OR, 2.684; 95% CI, 1.007–7.149; $P=0.048$) but not in those without IAB (OR, 0.753; 95% CI, 0.343–1.651; $P=0.479$).

Discussion

The present study found a significant interaction between IAB and low-risk PFO pertaining to CS risk. The results of the multiplicative interaction analysis and subgroup analysis indicated that isolated low-risk PFO was not associated with CS; however, when combined with IAB, low-risk PFO increased the risk of CS. The additive interaction results suggested that nearly 70% of the increased risk of CS associated with low-risk PFO was attributed to the interaction with IAB. Nevertheless, no significant multiplicative interaction between high-risk PFO and IAB was observed. Correspondingly, IAB was significantly associated with CS in patients with low-risk PFO, but not in those with high-risk PFO and without PFO.

PFO has been considered as an important risk factor for CS [1]. The prevalence of PFO is approximately 25% in the general population. Not all PFOs lead to stroke. Identifying high-risk PFOs is a crucial aspect of secondary prevention for patients with CS and may even serve as an important strategy for primary prevention. Currently, the diagnosis of PFO-associated strokes is primarily

Table 1 Characteristics of study population

	CS Group (N=256)	Control Group (N=156)	P value
Age (years)	56.7±9.7	53.7±13.0	0.014
Male	174 (68.0%)	85 (54.5%)	0.006
Body mass index (kg/m ²)	24.2±3.2	23.9±2.8	0.380
Alcohol	96 (37.5%)	39 (25.0%)	0.009
Smoking	76 (29.7%)	32 (20.5%)	0.040
Hypertension	155 (60.5%)	56 (35.9%)	<0.001
Diabetes	54 (21.1%)	12 (7.7%)	<0.001
CHD	8 (3.1%)	2 (1.3%)	0.332
Fibrinogen (g/L)	2.63±0.78	2.54±0.84	0.275
D-dimer (mg/L)	0.66±1.39	0.42±0.48	0.012
eGFR (mL/min)	97.0±13.4	98.5±14.7	0.287
HDL (mmol/L)	1.01±0.24	1.12±0.34	<0.001
LDL (mmol/L)	2.43±0.84	2.44±0.77	0.892
Homocysteine (umol/L)	12.70±10.41	11.41±9.98	0.233
LAD (mm)	34.5±4.5	33.1±4.6	0.02
RoPE score (point) ^a	3.63±1.43	4.36±1.66	<0.001
RoPE score >=6 ^a	26 (10.2%)	35 (22.4%)	0.001
P wave duration (ms)	117.4±12.1	113.0±13.1	0.001
IAB	123 (48.0%)	50 (32.1%)	0.001
PFO	127 (49.6%)	45 (28.8%)	<0.001
Low-risk PFO	38 (14.8%)	24 (15.4%)	0.894
High-risk PFO	89 (34.8%)	21 (13.5%)	<0.001

CHD coronary heart disease, CS cryptogenic stroke, eGFR estimated glomerular filtration rate, HDL high density lipoprotein, LAD left atrial dimension, LDL low density lipoprotein, PFO patent foramen ovale, IAB interatrial block

^a The RoPE score was calculated without incorporating the stroke imaging manifestation

Table 2 Morphometric and functional characteristics of PFO

	CS Group (N=127)	Control Group (N=45)	P value
RLS at rest			0.251
Grade 0	44 (34.6%)	15 (33.3%)	
Grade 1	52 (40.9%)	23 (51.1%)	
Grade 2	16 (12.6%)	6 (13.3%)	
Grade 3	15 (11.8%)	1 (2.2%)	
RLS after Valsalva maneuver			0.08
Grade 0	0	0	
Grade 1	33 (26.0%)	12 (26.7%)	
Grade 2	33 (26.0%)	19 (42.2%)	
Grade 3	61 (48.0%)	14 (31.1%)	
PFO height (mm)	2.59±1.37	1.99±0.85	0.001
Large-size PFO	70 (55.1%)	14 (31.1%)	0.006
Atrial septal aneurysm	19 (15.0%)	3 (6.7%)	0.152
Hypermobility septum	17 (13.4%)	3 (6.7%)	0.227

CS cryptogenic stroke, PFO patent foramen ovale, RLS right-to-left shunt

determined by clinical characteristics and the high-risk features of the PFO. In addition to clinical characteristics and the features of the PFO, the present study suggested that IAB was a neglected but important factor modifying the risk of PFO in CS and should be considered in clinical practice. There are several potential mechanisms underlying the interactions between PFO and IAB.

First, IAB may increase PFO-RLS, thereby raising the risk of paradoxical embolism associated with PFO. Although the mechanisms behind PFO-associated strokes are not fully understood, paradoxical embolism is considered a major contributing factor. PFO-RLS forms the basis of paradoxical embolism and stands as the most significant risk factor for PFO-associated strokes [1]. Factors leading to an increase in PFO-RLS, such as ASA, prominent Chiari network, and Eustachian valve, may increase CS risk [10]. Previously, researchers have focused primarily on the morphological factors of PFO that may lead to an increase in PFO-RLS. However, the impact of abnormal atrial electrical activity on PFO-RLS remains unclear. Normal atrial electrical activity originates from the sinoatrial node, and travels through the Bachmann bundle, interatrial septum, and coronary sinus to activate the left atrium. Therefore, the right atrium contracts earlier than the left atrium. When the right atrium contracts before the left, its pressure exceeds that of the left atrium, leading to PFO-RLS. Therefore, when IAB further delays the contraction of the left atrium, the risk of paradoxical embolism increases. A previous study reported that atrial mechanical dyssynchrony, a consequence of IAB, increased PFO-RLS [12]. Second, PFO may exacerbate the left atrial blood stasis caused by IAB. IAB itself is a risk factor for CS. The mechanisms underlying CS caused by IAB may be associated with left atrial blood stasis [5]. PFO-RLS may exert a significant effect on left atrial hemodynamics. A recent study reported that PFO-RLS may reduce stroke in the patients with AF by increasing left atrial appendage emptying velocity [13]. However, in a computational fluid dynamics study, PFO-RLS contributed to increased blood stasis in the left atrium [14]. Third, IAB may be associated with the risk of in situ thrombus formation in PFO. In addition to the paradoxical embolism, the PFO may also lead to in situ thrombus formation [3]. IAB may be associated with increased interatrial septal fat, a local marker of endothelial dysfunction and myocardial fibrosis [15, 16]. Therefore, IAB may be associated with the risk of in situ thrombus formation in PFO. Furthermore, IAB may also be associated with other risk factors of PFO-associated stroke, such as a hypermobile septum and left atrial enlargement [17, 18]. Overall, in

Table 3 Results of multivariable logistic regression models of cryptogenic stroke

Variates	Model 1		Model 2	
	OR (95%CI)	P value	OR (95%CI)	P value
Age (per 10 years)	1.211 (1.003, 1.463)	0.046	/	/
Male	1.702 (1.096, 2.644)	0.018	/	/
IAB	1.762 (1.132, 2.745)	0.012	2.023 (1.293, 3.165)	0.002
PFO				
Without PFO	Reference		Reference	
Low-risk PFO	1.402 (0.774, 2.542)	0.265	1.102 (0.597, 2.036)	0.756
High-risk PFO	3.930 (2.257–6.843)	< 0.001	3.791 (2.141, 6.710)	0.002
Hypertension	/	/	2.442 (1.562, 3.818)	0.000
Diabetes	/	/	2.524 (1.245, 5.114)	0.010
HDL (per mmol/L)	/	/	0.325 (0.144, 0.737)	0.007

CI confidence interval, HDL high density lipoprotein, OR odds ratio, PFO patent foramen ovale, IAB interatrial block

Model 1: adjusted for IAB, PFO, age and sex

Model 2: adjusted for IAB, PFO, age, sex, alcohol, smoking, hypertension, diabetes, fibrinogen, D-dimer, estimated glomerular filtration rate; homocysteine, high/low density lipoprotein and left atrial dimension

theory, a complex interaction may exist between the IAB and PFO in the causation of CS. Future studies are warranted to explore the potential mechanisms underlying the interaction between PFO and IAB.

In the present case–control study, we demonstrated a significant interaction between IAB and PFO in the development of CS. Similar to previous studies, the present study did not observe a significant association

between low-risk PFO and CS [1]. However, low-risk PFO increased the risk of CS approximately thrice in patients with IAB. This finding holds crucial clinical significance. Currently, the diagnosis of PFO-associated stroke is primarily based on clinical features and PFO morphology. In patients with low-risk PFO, the probability of PFO-associated stroke is usually considered low. However, based on our findings, we should not neglect

Table 4 Odds ratios and interaction analyses for cryptogenic stroke

Variates	Model 0		Model 1		Model 2	
	OR (95%CI)	P value	OR (95%CI)	P value	OR (95%CI)	P value
No-IAB/no-PFO	1 (reference)	/	1 (reference)	/	1 (reference)	/
No-IAB/low-risk PFO	0.732 (0.334, 1.606)	0.437	0.837 (0.375, 1.870)	0.665	0.529 (0.224, 1.250)	0.147
No-IAB/high-risk PFO	3.169 (1.652, 6.079)	0.001	3.352 (1.727, 6.504)	< 0.001	3.411 (1.709, 6.806)	0.001
IAB/no-PFO	1.590 (0.939, 2.692)	0.085	1.416 (0.827, 2.424)	0.205	1.424 (0.810, 2.505)	0.219
IAB/low-risk PFO	4.225 (1.635, 10.919)	0.003	3.804 (1.459, 9.918)	0.006	3.780 (1.416, 10.087)	0.008
IAB/high-risk PFO	5.650 (2.370, 13.469)	< 0.001	5.127 (2.133, 12.325)	< 0.001	5.450 (2.199, 13.504)	< 0.001
MI-1	3.653 (1.115, 12.506)	0.037	3.546 (1.096, 11.412)	0.046	4.291 (1.137, 16.191)	0.032
MI-2	1.204 (0.378, 3.841)	0.753	1.180 (0.365, 3.818)	0.782	1.101 (0.330, 3.672)	0.876
AP-1	0.684 (0.333, 1.050)	< 0.001	0.672 (0.299, 1.044)	< 0.001	0.709 (0.355, 1.063)	< 0.001
RERI-1	2.973 (-1.044, 6.989)	0.073	2.702 (-1.052, 6.455)	0.079	2.672 (-0.930, 6.273)	0.073
SI-1	8.984 (0.424, 190.576)	0.079	9.418 (0.278, 319.151)	0.106	28.968 (4*10 ⁻⁴ , 2*10 ⁶)	0.277
AP-2	0.396 (-0.217, 1.003)	0.101	0.334 (-0.351, 1.020)	0.169	0.322(-0.388, 1.031)	0.187
RERI-2	2.683 (-3.538, 8.905)	0.199	2.073 (-3.775, 7.920)	0.244	1.968 (-3.923, 7.860)	0.256
SI-2	1.867 (0.547, 3.369)	0.159	1.663 (0.466, 5.935)	0.217	1.624 (0.446, 5.912)	0.231

AP attributable portion, CI confidence interval, HDL high density lipoprotein, IAB interatrial block, MI multiplicative interaction between IAB and PFO, OR odds ratio, PFO patent foramen ovale, RERI relative excess risk due to interaction, SI synergy index of interaction, -1 interaction between IAB and low-risk PFO compared with no-PFO, -2 interaction between IAB and high-risk PFO compared with no-PFO

Model 0: including PFO, IAB and interaction terms

Model 1: Model 0 + age and sex

Model 2: Model 0 + age, sex, alcohol, smoking, hypertension, diabetes, fibrinogen, D-dimer, estimated glomerular filtration rate; homocysteine, high/low density lipoprotein and left atrial dimension

the significance of low-risk PFO in patients with IAB. With regard to high-risk PFO, similar to previous studies, we confirmed the significant association between high-risk PFO and CS. However, it was interesting that no significant interaction between IAB and high-risk PFO was detected. It was speculated that the strong association between high-risk PFO and CS might overshadow the role of interaction between high-risk PFO and IAB negligible. For example, the large RLS of high-risk RLS would dilute the impact of IAB on PFO-RLS, as mentioned above. To further explore the mechanism underlying the interaction between IAB and PFO, we assessed the correlation between IAB and the high-risk features of PFO, including PFO-RLS, ASA, and hypermobile septum, but no significant association was detected. While we did not demonstrate that IAB increases the PFO-RLS, it may still extend the duration of PFO-RLS. Whether this may increase the probability of paradoxical embolism requires further investigation. Furthermore, these results suggest that the interaction between IAB and PFO may be independent of PFO-RLS.

This study had several limitations. First, as a single-center study, the findings should be interpreted with caution and require further validation through multi-center studies. Second, the retrospective design introduces significant bias, particularly selection bias, since the study included only patients who underwent cTEE at our center, potentially resulting in a higher incidence of PFO compared to the general population. However, due to the low incidence of CS, conducting a prospective cohort study would be challenging. Despite these limitations, the primary aim of this study was to investigate the interaction between PFO and IAB. We demonstrated that IAB is not associated with PFO or its characteristics, minimizing the impact of selection bias on the assessment of the interaction. Additionally, subgroup analyses further validated the interaction between PFO and IAB. Lastly, we did not provide evidence for the mechanism underlying PFO and IAB interaction, thus warranting further investigation.

Conclusion

In summary, our study highlights the significant interaction between interatrial block (IAB) and patent foramen ovale (PFO) in cryptogenic strokes, mainly in those with low-risk PFO. These findings enhance our understanding of the mechanisms underlying CS and provide valuable insights into preventive measures.

Abbreviations

AF	Atrial fibrillation
AP	Attributable proportion
ASA	Atrial septal aneurysm

cTEE	Contrast transesophageal echocardiography
CI	Confidence intervals
CS	Cryptogenic stroke
IAB	Interatrial block
IS	Ischemic stroke
PFO	Patent foramen ovale
OR	Odds ratio
RLS	Right-to-left shunt flow
RERI	Relative excess risk due to interaction
SI	Synergy index
TIA	Transient ischemic attack

Supplementary Information

The online version contains supplementary material available at <https://doi.org/10.1186/s12883-024-03829-3>.

Supplementary Material 1.

Acknowledgements

None.

Authors' contributions

Conception and design: Ye Du, Buyun Xu, Yanxing Zhang, Yangbo Xing; administrative support: Buyun Xu; provision of study materials or patients: Ye Du, Yanxing Zhang, Yangbo Xing, Xiatian Liu, Huayong Jin; collection and assembly of data: Ye Du, Yanxing Zhang, Yuxin Zhang, Chengyi Li; data analysis and interpretation: Ye Du, Buyun Xu; manuscript writing: all authors; and final approval of the manuscript: all authors.

Funding

This work was supported by the Health Commission of Zhejiang Province, China (grant number: 2024KY481), and the Health Commission of Shaoxing, China (grant number: 2022KY031).

Availability of data and materials

The datasets analysed during the current study are available from the corresponding author on reasonable request.

Declarations

Ethics approval and consent to participate

The ethics review boards of Shaoxing People's Hospital approved this study, and the requirement for informed consent was waived owing to the retrospective nature of this study.

Consent for publication

Not applicable.

Competing interests

The authors declare no competing interests.

Received: 4 May 2024 Accepted: 27 August 2024

Published online: 14 September 2024

References

1. Tobis JM, Elgendy AY, Saver JL, et al. Proposal for updated nomenclature and classification of potential causative mechanism in patent foramen ovale-associated stroke. *JAMA Neurol.* 2020;77(7):878–86.
2. Diener HC, Easton JD, Hart RG, Kasner S, et al. Review and update of the concept of embolic stroke of undetermined source. *Nat Rev Neurol.* 2022;18(8):455–65.
3. Yan C, Li H, Wang C, et al. Frequency and size of in Situ Thrombus within patent foramen ovale. *Stroke.* 2023;54(5):1205–13.

4. Pristipino C, Sievert H, D'Ascenzo F, et al. European position paper on the management of patients with patent foramen ovale. General approach and left circulation thromboembolism. *Eur Heart J*. 2019;40(38):3182–95.
5. Power DA, Lampert J, Camaj A, et al. Cardiovascular complications of interatrial conduction block: JACC State-of-the-art review. *J Am Coll Cardiol*. 2022;79(12):1199–211.
6. Lampert J, Power D, Havaladar S, et al. Interatrial Block Association with adverse cardiovascular outcomes in patients without a history of atrial fibrillation. *JACC Clin Electrophys*. 2023;9(8):1804.
7. Lee PH, Song JK, Kim JS, et al. Cryptogenic stroke and high-risk patent foramen ovale: The DEFENSE-PFO trial. *J Am Coll Cardiol*. 2018;71(20):2335–42.
8. Heidenreich PA, Bozkurt B, Aguilar D, et al. 2022 AHA/ACC/HFSA Guideline for the management of heart failure: a report of the American College of Cardiology/American Heart Association Joint Committee on Clinical Practice Guidelines. *J Am Coll Cardiol*. 2022;79(17):1757–80.
9. Zhu J, Chen A, Zhu L, et al. Calf muscle pump tensing as a novel maneuver to improve the diagnostic performance of detecting patent foramen ovale during transesophageal echocardiography. *Front Neurol*. 2023;14:1116764.
10. Holda MK, Krawczyk-Ożóg A, Koziej M, et al. Patent foramen ovale channel morphometric characteristics associated with cryptogenic stroke: the MorPFO score. *J Am Soc Echocardiogr*. 2021;34(12):1285–93.
11. Källberg H, Ahlbom A, Alfredsson L. Calculating measures of biological interaction using R. *Eur J Epidemiol*. 2006;21(8):571–3.
12. Mahfouz RA, Alawady WS, Salem A, Abdelghafar AS. Atrial dyssynchrony and left atrial stiffness are risk markers for cryptogenic stroke in patients with patent foramen ovale. *Echocardiography*. 2017;34(12):1888–94.
13. Baik M, Shim CY, Gwak SY, et al. Patent foramen ovale may decrease the risk of left atrial thrombosis in stroke patients with atrial fibrillation. *J Stroke*. 2023;25(3):417–20.
14. Rigatelli G, Zuin M, Roncon L. Increased blood residence time as markers of high-risk patent foramen ovale. *Transl Stroke Res*. 2023;14(3):304–10.
15. Samanta R, Houbois CP, Massin SZ, Seidman M, et al. Interatrial septal fat contributes to interatrial conduction delay and atrial fibrillation recurrence following ablation. *Circ Arrhythmia Electrophys*. 2021;14(10):E010235.
16. Shaihov-Teper O, Ram E, Ballan N, et al. Extracellular vesicles from epicardial fat facilitate atrial fibrillation. *Circulation*. 2021;143(25):2475–93.
17. Nakayama R, Takaya Y, Akagi T, et al. Identification of high-risk patent foramen ovale associated with cryptogenic stroke: development of a scoring system. *J Am Soc Echocardiogr*. 2019;32(7):811–6.
18. Rigatelli G, Zuin M, Adami A, et al. Left atrial enlargement as a maker of significant high-risk patent foramen ovale. *Int J Cardiovasc Imaging*. 2019;35(11):2049–56.

Publisher's Note

Springer Nature remains neutral with regard to jurisdictional claims in published maps and institutional affiliations.